2017

From the Circle to the Square: Symmetry and Degeneracy in Quantum Mechanics

Dahyeon Lee
Oberlin College

From the Circle to the Square: Symmetry and Degeneracy in Quantum Mechanics

Dahyeon Lee
Department of Physics and Astronomy,
Oberlin College

March 31, 2017

Executive Summary

The relationship between degeneracy and symmetry in quantum mechanics is explored using two dimensional infinite potential wells with boundaries $|x|^n + |y|^n = a^n$ for $n \geq 2$, whose limiting cases are circular ($n = 2$) and square ($n \to \infty$) well. Analytic solutions for the circular and square cases are derived from separation of variables.

Boundary element method (BEM) is a numerical method that solves PDEs using boundary conditions. The BEM is used to solve potential well problems. The method is first tested by comparing numerical solutions with analytic solutions for the circular and square wells. For the ground state of the circular well, the error as a function of the number of discretization points N decreased like $1/N^2$.

As the potential well changed shape from circle to square, energy eigenvalues and degeneracies are tracked. Energy levels split (when degeneracies are lifted), merge, and cross.

I thank Dan Styer for all the insights and life lessons he has given me.

Contents

Chapter 1

Introduction

What is the relationship between symmetry and degeneracy in quantum mechanics? Emmy Noether approached this question using very powerful and general formal techniques.[1] The abstractions of Noether's approach is both blessing and curse – while the approach is highly general, it is also difficult to see "what's going on" in any concrete way.

This thesis approaches the same question in a specific, concrete, visualizable manner, through a particular two-dimensional potential.

In two dimensions, the solutions for the infinite square well and infinite circular well can be found analytically. For the infinite square well, the solution is a simple extension to the one dimensional case. For the infinite circular well, separation of variables in polar coordinates gives the answer.

But we have no analytic solutions for potentials whose shapes are somewhere in between perfectly circular and perfectly square. For example, a potential well with the boundary $x^4 + y^4 = a^4$ does not have an analytic solution through separation of variables. In order to find energy eigenvalues and eigenfunctions for such potentials, we use numerical methods.

The boundary element method (BEM) numerically solves partial differential equations by discretizing the boundary of the region of interest. In the context of two dimensional quantum mechanics eigenproblem, the boundary is the potential wall and the partial differential equation to be solved is the time-independent Schrödinger equation. Given a set of boundary conditions, the BEM finds the solution to the partial differential equation by calculating the contribution of each boundary element to the solution inside the region.

[1] Dwight E. Neuenschwander *Emmy Noether's Wonderful Theorem* (Johns Hopkins University Press, Baltimore, 2011).

We first determine the accuracy of the numerical solutions found by BEM as a function of discretization points, by comparing the BEM result to analytic solutions for circular and square wells. We then apply BEM to potential wells of the type $x^n + y^n = a^n$, which allows us to see how the energy eigenvalues and eigenfunctions behave as we interpolate smoothly from circle to square.

Chapter 2

Potential Wells

2.1 2-D infinite square well

For the one-dimensional infinite square well with potential

$$V(x) = \begin{cases} 0 & \text{if } 0 < x < a \\ \infty & \text{otherwise ,} \end{cases}$$

the stationary states are

$$\psi_n(x) = \sqrt{\frac{2}{a}} \sin\left(\frac{n\pi}{a}x\right) \tag{2.1}$$

with the energies

$$E_n = \frac{n^2\pi^2\hbar^2}{2ma^2} \ . \tag{2.2}$$

In the two-dimensional case where

$$V(x,y) = \begin{cases} 0 & \text{if } 0 < x < a \text{ and } 0 < y < a \\ \infty & \text{otherwise ,} \end{cases}$$

we can generalize the solution from the one-dimensional case to two dimensions using separation of variables.

Assume that the solution can be written as $\psi(x,y) = X(x)Y(y)$. The time-independent Schrödinger equation inside the potential well is

$$-\frac{\hbar^2}{2m}\left(\frac{\partial^2\psi(x,y)}{\partial x^2} + \frac{\partial^2\psi(x,y)}{\partial y^2}\right) = E\psi(x,y) \ . \tag{2.3}$$

Using separation of variables,

$$-\frac{\hbar^2}{2m}\left(Y(y)\frac{\partial^2 X(x)}{\partial x^2}+X(x)\frac{\partial^2 Y(y)}{\partial y^2}\right)=EX(x)Y(y)\ . \tag{2.4}$$

Dividing both sides by XY and rearranging,

$$\frac{1}{X}\frac{\partial^2 X}{\partial x^2}=-\frac{1}{Y}\frac{\partial^2 Y}{\partial y^2}-\frac{2mE}{\hbar^2}\ . \tag{2.5}$$

The left hand side of the equation is a function of x and the right hand side depends only on y. Thus, they should both equal to a constant, say $-k_x^2$ (some negative number). This choice will be justified in a moment. We now have two ordinary differential equations:

$$\frac{1}{X}\frac{\partial^2 X}{\partial x^2}=-k_x^2\ , \tag{2.6}$$

$$\frac{1}{Y}\frac{\partial^2 Y}{\partial y^2}=k_x^2-\frac{2mE}{\hbar^2}\equiv -k_y^2\ , \tag{2.7}$$

where k_y is defined so that

$$E=\frac{\hbar^2}{2m}(k_x^2+k_y^2)\ . \tag{2.8}$$

The first differential equation has solutions of the form

$$X(x)=A\sin(k_x x)+B\cos(k_x x)\ . \tag{2.9}$$

Using the boundary condition $X(0)=X(a)=0$ and choosing the appropriate normalization constant,

$$X(x)=\sqrt{\frac{2}{a}}\sin\left(\frac{n_x\pi}{a}x\right)\ , \tag{2.10}$$

where $n_x=1,2,3,\ldots$ and $k_x=n_x\pi/a$.

Note that if we had chosen $+k_x^2$ (some positive number) instead of $-k_x^2$ as our constant, the general solution would have been

$$X(x)=Ae^{k_x x}+Be^{-k_x x}\ , \tag{2.11}$$

which cannot satisfy the boundary conditions.

Similarly for $Y(y)$,

$$Y(y)=\sqrt{\frac{2}{a}}\sin\left(\frac{n_y\pi}{a}y\right)\ . \tag{2.12}$$

Combining the results for the x and y equations,

$$\psi(x,y)=X(x)Y(y)=\frac{2}{a}\sin\left(\frac{n_x\pi}{a}x\right)\sin\left(\frac{n_y\pi}{a}y\right)\ , \tag{2.13}$$

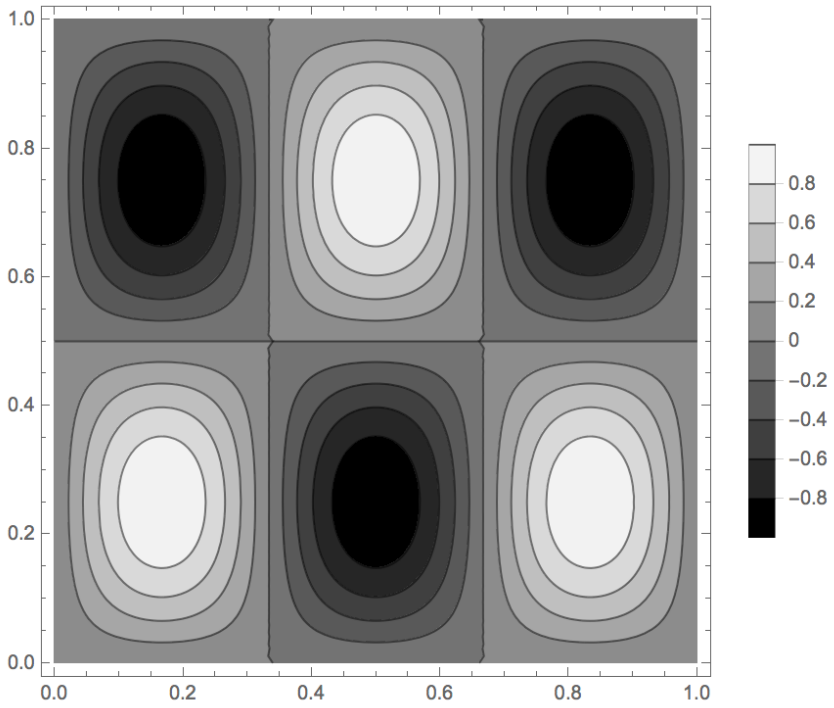

Figure 2.1: Energy eigenstate for the two-dimensional infinite square well, for $n_x = 3$ and $n_y = 2$. The size of the well is 1×1. There are three columns and two rows of bumps. In general, the eigenstate will look like a grid of $n_x \times n_y$ bumps.

$$E(n_x, n_y) = \frac{(n_x^2 + n_y^2)\pi^2\hbar^2}{2ma^2} \ . \tag{2.14}$$

We can intuitively understand the shapes of the energy eigenstates. Take, for example, the case where $n_x = 3$ and $n_y = 2$. The corresponding energy eigenstate is

$$\psi_{3,2}(x, y) = \frac{2}{a} \sin\left(\frac{3\pi}{a}x\right) \sin\left(\frac{2\pi}{a}y\right) \ . \tag{2.15}$$

Figure 2.1 shows the contour plot for $\psi_{3,2}$. There are three "bumps" along the x axis and two bumps along the y axis. Any combination of (n_x, n_y) will yield an eigenstate with n_x columns and n_y rows of bumps.

The eigenenergy in (2.14) is proportional to $n_x^2 + n_y^2$. The first few eigenenergies are shown in Table 2.1 along with corresponding n_x and n_y.

Eigenenergy	n_x	n_y	$n_x^2 + n_y^2$
E_{11}	1	1	2
E_{12}	1	2	5
E_{22}	2	2	8
E_{13}	1	3	10
E_{23}	2	3	13
E_{14}	1	4	17
E_{33}	3	3	18
E_{24}	2	4	20

Table 2.1: The first 8 eigenenergies for the two dimensional infinite square well. $E_{n_x n_y} = (n_x^2 + n_y^2)\pi^2\hbar^2/(2ma^2)$ is proportional to $n_x^2 + n_y^2$.

Note that states with $n_x \neq n_y$ are doubly degenerate. For example, $E_{13} = E_{31}$ and the corresponding eigenstates $\psi_{3,1}$ and $\psi_{1,3}$ are linearly independent, which makes E_{13} doubly degenerate.

2.2 Infinite circular well

We define the infinite circular well of radius a with the potential

$$V(r, \theta) = V(r) = \begin{cases} 0 & \text{if } r < a \\ \infty & \text{if } r \geq a \ . \end{cases} \tag{2.16}$$

The Schrödinger equation inside the well is

$$-\frac{\hbar^2}{2m}\nabla^2\psi(r,\theta) = E\psi(r,\theta) \ , \tag{2.17}$$

or,

$$-\frac{\hbar^2}{2m}\left(\frac{\partial^2}{\partial r^2} + \frac{1}{r}\frac{\partial}{\partial r} + \frac{1}{r^2}\frac{\partial^2}{\partial\theta^2}\right)\psi(r,\theta) = E\psi(r,\theta) \ . \tag{2.18}$$

Using the usual separation of variables, substitute $\psi(r,\theta) = R(r)\Theta(\theta)$ and get

$$-\frac{\hbar^2}{2m}\left(\Theta\frac{\partial^2 R}{\partial r^2} + \frac{\Theta}{r}\frac{\partial R}{\partial r} + \frac{R}{r^2}\frac{\partial^2\Theta}{\partial\theta^2}\right) = ER\Theta \ . \tag{2.19}$$

With some rearrangement,

$$-\frac{1}{\Theta}\frac{\partial^2\Theta}{\partial\theta^2} = \frac{r^2}{R}\frac{\partial^2 R}{\partial r^2} + \frac{r}{R}\frac{\partial R}{\partial r} + \frac{2mE}{\hbar^2}r^2 \ . \tag{2.20}$$

The left hand side depends only on θ and the right hand side depends only on r, so they must both be a constant. Let's call the constant l^2 (some positive number). We choose a positive constant because a negative constant cannot satisfy the boundary condition $\Theta(\theta) = \Theta(\theta + 2\pi)$. This leads to two ordinary differential equations:

$$\frac{\partial^2\Theta}{\partial\theta^2} = -l^2\Theta \ , \tag{2.21}$$

$$r^2\frac{\partial^2 R}{\partial r^2} + r\frac{\partial R}{\partial r} + (k^2r^2 - l^2)R = 0 \ , \tag{2.22}$$

where $k = \sqrt{2mE}/\hbar$.

The first equation is easier to solve. The general solution is

$$\Theta(\theta) = A\sin(l\theta) + B\cos(l\theta) \tag{2.23}$$

with two linearly independent solutions

$$\Theta(\theta) = C\sin(l\theta) \quad \text{or} \quad \Theta(\theta) = C\cos(l\theta) \ . \tag{2.24}$$

The boundary condition $\Theta(\theta) = \Theta(\theta + 2\pi)$ restricts l to be integers, $l = 0, \pm1, \pm2, \cdots$.

The radial equation seems more complicated, but this is the well-known *Bessel equation*. The general solution is

$$R(r) = AJ_{|l|}(kr) + BY_{|l|}(kr) \ , \tag{2.25}$$

where $J_l(kr)$ is the lth order Bessel function of the first kind and $Y_l(kr)$ is the lth order Bessel function of the second kind. The Bessel functions of the second kind diverge at $r = 0$ and thus cannot be normalized. We must therefore have $B = 0$ in order to get normalizable solutions, which leads to

$$R(r) = AJ_{|l|}(kr) \ . \tag{2.26}$$

The boundary condition $R(a) = 0$ becomes $J_{|l|}(ka) = J_{|l|}(a\sqrt{2mE}/\hbar) = 0$. If we designate the nth root of $J_{|l|}$ as z_{nl}, then

$$E_{nl} = \frac{z_{nl}^2\hbar^2}{2ma^2} \ . \tag{2.27}$$

The corresponding eigenstates are linear combinations of

$$\psi_{nl}(r,\theta) = C_{nl}J_{|l|}(kr)\sin(l\theta) \quad \text{and} \quad \psi_{nl}(r,\theta) = C_{nl}J_{|l|}(kr)\cos(l\theta) \ , \tag{2.28}$$

where C_{nl} is the appropriate normalization constant. There are in fact infinitely many solutions, but there are only two linearly independent solutions, which means that the solution is doubly degenerate (except for the case $l = 0$, which is not degenerate).[1] Note that since linear combinations of sines and cosines with the same argument just introduce a phase shift, the infinitely many solutions are simple rotations of either $C_{nl}J_{|l|}(kr)\sin(l\theta)$ or $C_{nl}J_{|l|}(kr)\cos(l\theta)$.

Figure 2.2 shows the energy eigenfunctions for various values of n and l. The number of radial nodes is $n - 1$ and the number of angular nodes is $2l$. In the case where $n = 1$ and $l = 0$ (Figure 2.2a – the ground state), there is no node. When $n = 2$ and $l = 3$ (Figure 2.2d), there are six angular nodes and one radial node.

2.3 From circular well to square well

This project investigates potential wells that are neither perfectly square nor perfectly circular, but somewhere in between. An example of such a potential would be one whose boundary is $x^4+y^4 = 1$, shown in Figure 2.3a.[2] Any type of boundary of the form $x^n + y^n = 1$ works, where $n > 2$ and need not be an integer. Figure 2.3 shows potential wells with the boundary $x^n + y^n = 1$ for different

[1] Another potential source of degeneracy is the fact that l can assume both positive and negative integer values. In particular, $\psi_{n,l}$ has the same energy as $\psi_{n,-l}$. However, this does not contribute anything to degeneracy because the solutions for each case just differ by a sign in the first case of (2.28) and are identical in the second case. They are not linearly independent to the solutions in (2.28).

[2] x and y here are scaled variables: x/a becomes x and y/a becomes y. For the remainder of this thesis, we use scaled variables.

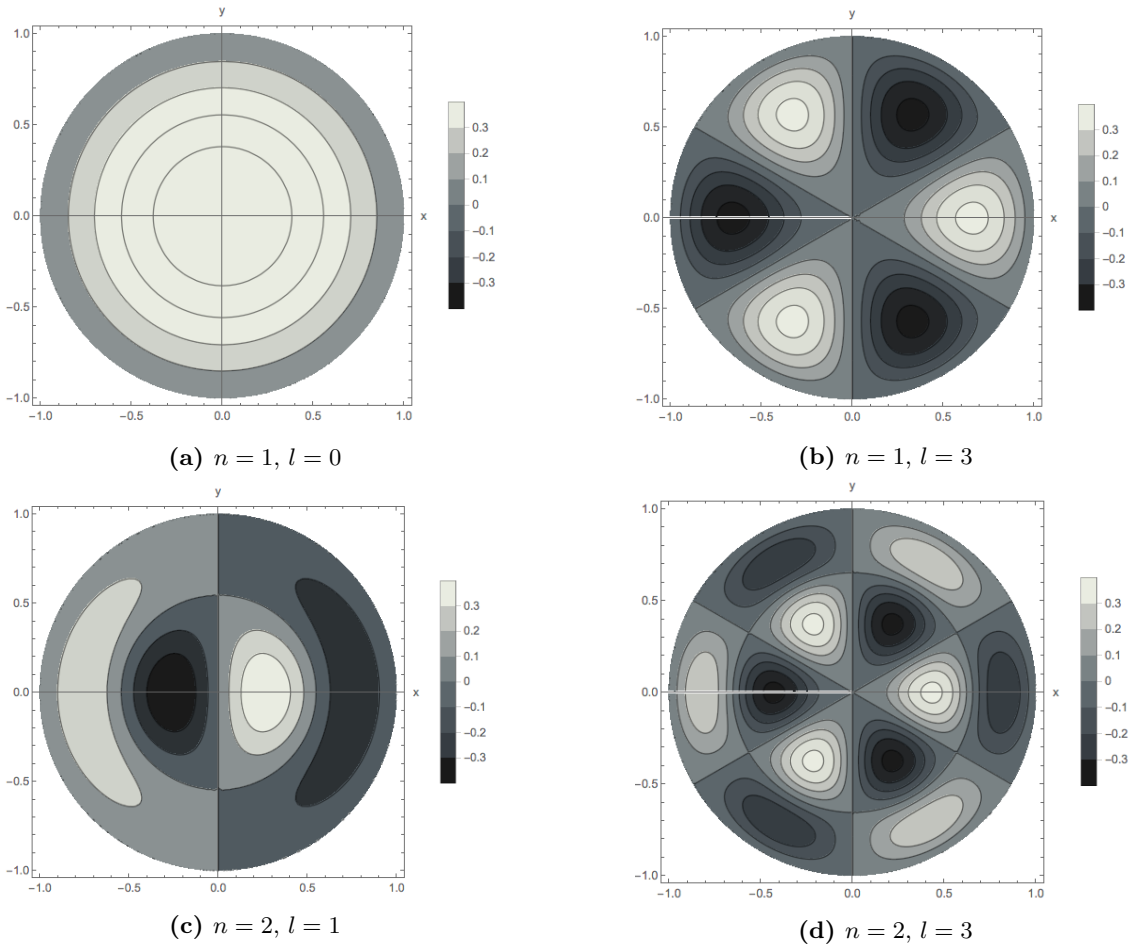

(a) $n = 1$, $l = 0$ **(b)** $n = 1$, $l = 3$

(c) $n = 2$, $l = 1$ **(d)** $n = 2$, $l = 3$

Figure 2.2: Contour plots of energy eigenfunctions for the infinite circular well of radius 1, corresponding to various quantum numbers n and l.

values of n. As n increases from 2 to larger values, the boundary transforms from perfectly circlular to square.

There is one complication, however. For equations like $x^3 + y^3 = 1$, the graph is not a closed curve. It decreases like a linear function on the second and fourth quadrants. In order to get the desired potential well, we need to take the function in the first quadrant and reflect it with respect to the x and y axes to get a closed boundary. In other words, the equation is $|x|^3 + |y|^3 = 1$.

We have found analytic solutions to the Schrödinger equation for the square and circular potential wells. Separation of variables by writing $\psi(x, y) = X(x)Y(y)$ or $\psi(r, \theta) = R(r)\Theta(\theta)$ proved to be useful. For potential wells that are neither circular nor square, separation of variables cannot be used. If we try to write $\psi(x, y) = X(x)Y(y)$, the boundary condition for $X(x)$ depends on y. Same

goes for separation of variables of the form $\psi(r, \theta) = R(r)\Theta(\theta)$. As a result, $X(x)$ and $R(r)$ will invariably depend on y and θ, which contradicts the assumption that the solution can be written as a product of functions of just one variable.

Instead, we need to use numerical methods to find solutions for this type of potential. One such method is the Boundary Element Method (BEM), explained in the next chapter.

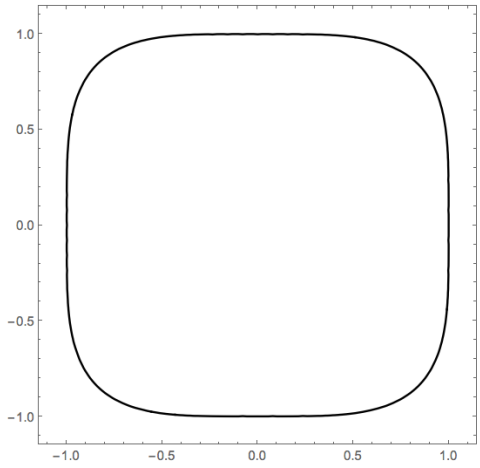

(a) $x^4 + y^4 = 1$

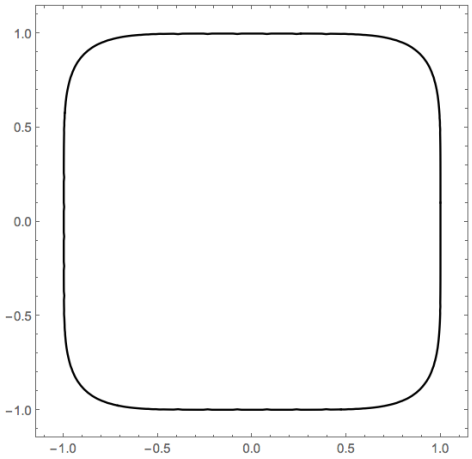

(b) $x^6 + y^6 = 1$

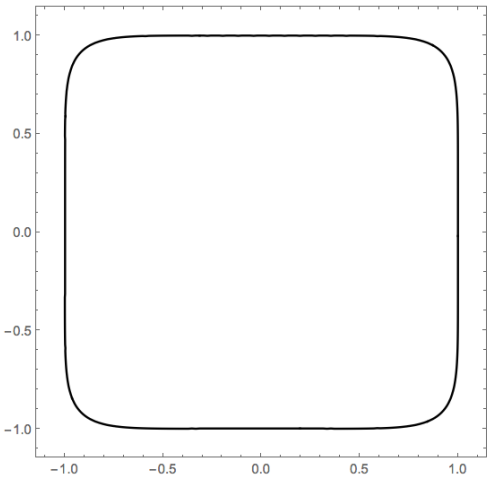

(c) $x^8 + y^8 = 1$

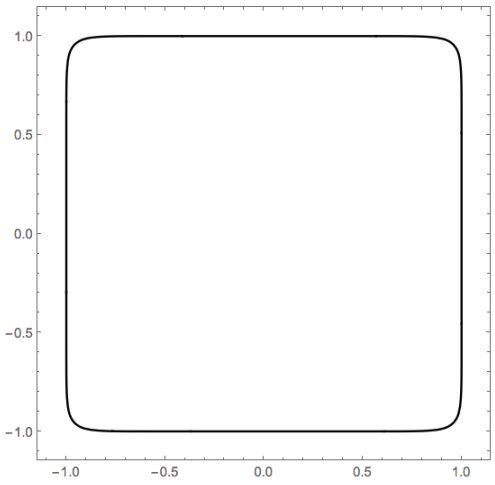

(d) $x^{16} + y^{16} = 1$

Figure 2.3: Potential wells with the boundary $x^n + y^n = 1$. As n gets bigger, the boundary looks more and more like a square. Analytic solutions for this type of potential cannot be found.

Chapter 3

Boundary Element Method (BEM)

The Boundary Element Method (BEM) is a numerical method that is useful for problems where the Green's function is available. A good example is the two-dimensional potential well problem. The BEM allows us to write the wavefunction inside the potential well as a line integral of its normal derivative and the Green's function along the boundary, as we will soon see. The BEM is useful because there is no need to discretize the entire region of interest. Only the boundary of the region need be discretized for numerical evaluation.

Before going into details of the BEM, let us begin by setting up the infinite potential well problem in the most general way. The potential well is defined as

$$V(x,y) = \begin{cases} 0 & \text{if } (x,y) \in D \\ \infty & \text{if } (x,y) \notin D \ , \end{cases} \tag{3.1}$$

where D is the region of interest. For convenience, we write the boundary of D as ∂D. We are also given the boundary condition

$$\psi(x,y) = 0 \quad \text{if } (x,y) \in \partial D \ . \tag{3.2}$$

Inside the region D, the particle obeys the Schrödinger equation:

$$-\frac{\hbar^2}{2m}\left(\frac{\partial^2\psi(x,y)}{\partial x^2} + \frac{\partial^2\psi(x,y)}{\partial y^2}\right) = E\psi(x,y) \ . \tag{3.3}$$

Our task is to find the solutions to (3.3) under the boundary condition (3.2).

3.1 Reciprocal relationship

Assume that we have two solutions to (3.3) and call them ψ_1 and ψ_2. We will show that

$$\int_{\partial D} \left(\psi_2 \frac{\partial \psi_1}{\partial n} - \psi_1 \frac{\partial \psi_2}{\partial n} \right) ds = 0 \ , \tag{3.4}$$

where $\partial/\partial n$ is the normal derivative. Equation (3.4) is called the *reciprocal relation*. The proof requires the divergence theorem: for some vector field in the region D with boundary ∂D

$$\mathbf{F} = u(x,y)\,\hat{\mathbf{i}} + v(x,y)\,\hat{\mathbf{j}} \ ,$$

we can write

$$\int_{\partial D} \mathbf{F} \cdot \hat{\mathbf{n}} \; ds(x,y) = \iint_D \nabla \cdot \mathbf{F} \, dx \, dy \ , \tag{3.5}$$

where $\hat{\mathbf{n}} = n_x\,\hat{\mathbf{i}} + n_y\,\hat{\mathbf{j}}$ is the unit normal vector. Evaluating the dot products, we can rewrite the divergence theorem as

$$\int_{\partial D} (u n_x + v n_y)\, ds(x,y) = \iint_D \left(\frac{\partial u}{\partial x} + \frac{\partial v}{\partial y} \right) dx \, dy \ . \tag{3.6}$$

Meanwhile, since ψ_1 and ψ_2 are solutions to equation (3.3),

$$-\frac{\hbar^2}{2m} \left(\frac{\partial^2 \psi_1}{\partial x^2} + \frac{\partial^2 \psi_1}{\partial y^2} \right) = E\psi_1 \ , \tag{3.7}$$

$$-\frac{\hbar^2}{2m} \left(\frac{\partial^2 \psi_2}{\partial x^2} + \frac{\partial^2 \psi_2}{\partial y^2} \right) = E\psi_2 \ . \tag{3.8}$$

Multiply the first equation by ψ_2 and the second by ψ_1 and take the difference to get

$$\psi_2 \frac{\partial^2 \psi_1}{\partial x^2} - \psi_1 \frac{\partial^2 \psi_2}{\partial x^2} + \psi_2 \frac{\partial^2 \psi_1}{\partial y^2} - \psi_1 \frac{\partial^2 \psi_2}{\partial y^2} = 0 \ , \tag{3.9}$$

which can be written as

$$\frac{\partial}{\partial x} \left(\psi_2 \frac{\partial \psi_1}{\partial x} - \psi_1 \frac{\partial \psi_2}{\partial x} \right) + \frac{\partial}{\partial y} \left(\psi_2 \frac{\partial \psi_1}{\partial y} - \psi_1 \frac{\partial \psi_2}{\partial y} \right) = 0 \ . \tag{3.10}$$

This can be integrated over D:

$$\iint_D \left[\frac{\partial}{\partial x} \left(\psi_2 \frac{\partial \psi_1}{\partial x} - \psi_1 \frac{\partial \psi_2}{\partial x} \right) + \frac{\partial}{\partial y} \left(\psi_2 \frac{\partial \psi_1}{\partial y} - \psi_1 \frac{\partial \psi_2}{\partial y} \right) \right] dx \, dy = 0 \ . \tag{3.11}$$

Now apply the divergence theorem to find

$$\int_{\partial D} \left[\left(\psi_2 \frac{\partial \psi_1}{\partial x} - \psi_1 \frac{\partial \psi_2}{\partial x} \right) n_x + \left(\psi_2 \frac{\partial \psi_1}{\partial y} - \psi_1 \frac{\partial \psi_2}{\partial y} \right) n_y \right] ds = 0 \ , \tag{3.12}$$

which is the same as

$$\int_{\partial D} \left(\psi_2 \nabla \psi_1 \cdot \hat{\mathbf{n}} - \psi_1 \nabla \psi_2 \cdot \hat{\mathbf{n}} \right) ds = 0 \ , \tag{3.13}$$

or, using the definition of directional derivative,

$$\int_{\partial D} \left(\psi_2 \frac{\partial \psi_1}{\partial n} - \psi_1 \frac{\partial \psi_2}{\partial n} \right) ds = 0 \ . \tag{3.14}$$

This is the reciprocal relation that we were looking for.

3.2 Green's function

The Green's function is a function of two points, say (ξ, η) and (x, y), which we write $G(x, y; \xi, \eta)$. It plays a central role in the BEM because combined with the reciprocal relationship, Green's function allows us to compute the eigenstates of the potential well from the relation

$$\psi(\xi, \eta) = \frac{\hbar^2}{m} \int_{\partial D} \left[\psi(x, y) \frac{\partial}{\partial n} G(x, y; \xi, \eta) - G(x, y; \xi, \eta) \frac{\partial}{\partial n} \psi(x, y) \right] ds \ , \tag{3.15}$$

which we will derive in the next section.

The Green's function for the Schrödinger equation is defined as the solution of

$$\left[E - \hat{H}(\mathbf{r}) \right] G(\mathbf{r}; \mathbf{r}') = \delta(\mathbf{r} - \mathbf{r}') \ , \tag{3.16}$$

where $\mathbf{r}$ and $\mathbf{r}'$ are some points in D. Written in this way, it is hard to grasp the physical meaning of Green's function. In order to gain a better understanding, let us plug in the Hamiltonian for our potential well, namely $-\frac{\hbar^2}{2m} \nabla^2$.

$$\left(\nabla^2 + k^2 \right) G(\mathbf{r}; \mathbf{r}') = \frac{2m}{\hbar^2} \delta(\mathbf{r} - \mathbf{r}') \ , \tag{3.17}$$

where $k = \sqrt{2mE}/\hbar$ as usual. This is very similar to the free particle Schrödinger equation where $V(\mathbf{r}) = 0$ everywhere:

$$\left(\nabla^2 + k^2 \right) \psi(\mathbf{r}) = 0 \ . \tag{3.18}$$

In fact, if we have a spike in the potential at $\mathbf{r}'$ such that $V(\mathbf{r}) = \delta(\mathbf{r} - \mathbf{r}')$, then the Schrödinger equation becomes

$$\left(\nabla^2 + k^2\right)\psi(\mathbf{r}) = \delta(\mathbf{r} - \mathbf{r}')\psi(\mathbf{r}) \ , \tag{3.19}$$

which is the same as (3.17) except for the $\psi(\mathbf{r})$ on the right hand side.

From this connection, we infer that the Green's function $G(\xi, \eta, x, y)$ is the solution to the Schrödinger equation when the potential is zero everywhere except at $\mathbf{r}'$. And at $\mathbf{r}'$, the potential is infinite. This interpretation is useful because we can write

$$V(\mathbf{r}) = \int V(\mathbf{r}')\delta(\mathbf{r} - \mathbf{r}')\, d\mathbf{r}' \ , \tag{3.20}$$

where the integral is over all space. Using this property, the Schrödinger equation can be written as

$$\begin{aligned}\left(\nabla^2 + k^2\right)\psi(\mathbf{r}) &= V(\mathbf{r})\psi(\mathbf{r}) \\ &= \int V(\mathbf{r}')\delta(\mathbf{r} - \mathbf{r}')\psi(\mathbf{r})\, d\mathbf{r}'\end{aligned} \tag{3.21}$$

If we can somehow find the solution for the case where the right hand side is just $\delta(\mathbf{r}-\mathbf{r}')$ (definition of Green's function), then we are done because we can think of the given potential as an addition of delta functions according to (3.20). The solution would be just a sum of Green's functions corresponding to each delta function.[1]

The Green's function for two-dimensional Schrödinger equation is[2]

$$G(\mathbf{r}; \mathbf{r}') = -\frac{im}{2\hbar^2} H_0^{(1)}(k\left|\mathbf{r} - \mathbf{r}'\right|) \ . \tag{3.22}$$

$H_0^{(1)}$ is the zeroth order *Hankel function* of the first kind, defined as a linear combination of Bessel functions of the first and second kinds in the following way:

$$H_n^{(0)}(z) \equiv J_n(z) + iY_n(z) \ . \tag{3.23}$$

[1]This reasoning works because if ψ_1 solves the Schrödinger equation for $V_1(\mathbf{r}) = V_{0,1}\delta(\mathbf{r} - \mathbf{r}')$ and ψ_2 solves the Schrödinger equation for $V_2(\mathbf{r}) = V_{0,2}\delta(\mathbf{r} - \mathbf{r}')$, then $\psi_1 + \psi_2$ solves the Schrödinger equation for $V_1(\mathbf{r}) + V_2(\mathbf{r})$. For potentials that are not delta functions, this is not true.

[2]See, for example, Kosztin, I., Schulten, K. "Boundary integral method for stationary states of two-dimensional equation systems," *International Journal of Modern Physics C* **8** 293–325 (April 1997)

3.3 Finding eigenstates

With the reciprocal relation and Green's function, we are now ready to derive (3.15). There are three cases: first, consider the case $(\xi, \eta) \notin D$. Notice that from equation (3.17), $G(\mathbf{r}; \mathbf{r}') = G(x, y; \xi, \eta)$ is the solution to the free particle Schrödinger equation (3.18) everywhere except at (ξ, η). Since $(\xi, \eta) \notin D$, $G(x, y; \xi, \eta)$ is a solution to the free particle Schrödinger equation everywhere on D (Figure 3.1a). And because $G(x, y; \xi, \eta)$ is a solution to our PDE everywhere on D, we can use the reciprocal relation with another unknown solution $\psi(x, y)$:

$$\int_{\partial D} \left[\psi(x,y) \frac{\partial}{\partial n} G(x,y;\xi,\eta) - G(x,y;\xi,\eta) \frac{\partial}{\partial n} \psi(x,y) \right] ds = 0 \quad \text{if } (\xi,\eta) \notin D \ . \tag{3.24}$$

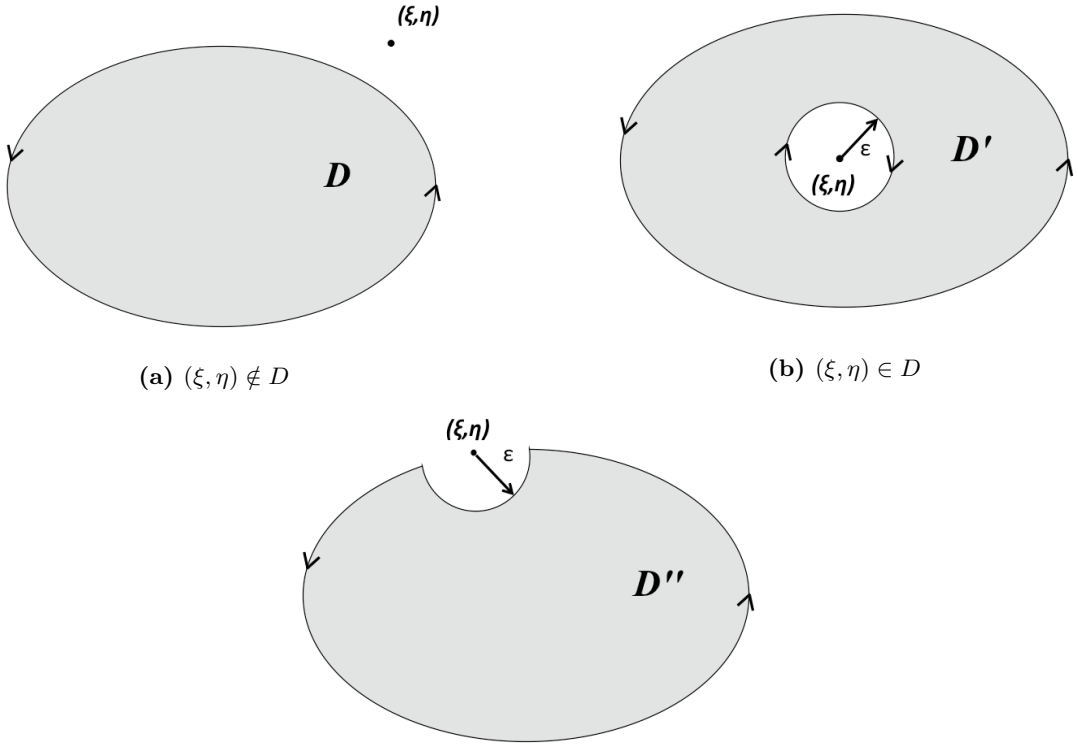

(a) $(\xi, \eta) \notin D$

(b) $(\xi, \eta) \in D$

(c) $(\xi, \eta) \in \partial D$

Figure 3.1: Three possibilities to consider when applying the reciprocal relations.

Second, consider the case where $(\xi, \eta) \in D$. We cannot apply the reciprocal relation to $G(\xi, \eta, x, y)$ on D because the Green's function does not satisfy the free particle Schrödinger equation at (ξ, η). In order to fix this problem, we make a disk of radius ϵ centered at (ξ, η) and redefine

the domain so that the disk is excluded from it, and call the new domain D' (Figure 3.1b). The boundary of D', which we will call $\partial D'$, has two parts: ∂D (the outer curve) and ∂D_ϵ (boundary of the inner disk). The orientation of the boundary is chosen so that the region D' is always on the left as one moves along the curve.[3] With this orientation, the normal vectors always point away from D', i.e. outward on the outer curve and inward on the inner curve. Since $G(x,y;\xi,\eta)$ satisfies our PDE everywhere on D', the reciprocal relation can be used for $G(x,y;\xi,\eta)$ and some unknown solution $\psi(x,y)$:

$$\int\limits_{\partial D'} \left(\psi\frac{\partial G}{\partial n} - G\frac{\partial \psi}{\partial n}\right) ds = \int\limits_{\partial D} \left(\psi\frac{\partial G}{\partial n} - G\frac{\partial \psi}{\partial n}\right) ds + \int\limits_{\partial D_\epsilon} \left(\psi\frac{\partial G}{\partial n} - G\frac{\partial \psi}{\partial n}\psi\right) ds = 0 \ . \tag{3.25}$$

Since this must hold for any disk of radius ϵ, take the limit $\epsilon \to 0^+$.

$$\int\limits_{\partial D} \left(\psi\frac{\partial G}{\partial n} - G\frac{\partial \psi}{\partial n}\right) ds = -\lim_{\epsilon\to 0^+} \int\limits_{\partial D_\epsilon} \left(\psi\frac{\partial G}{\partial n} - G\frac{\partial \psi}{\partial n}\right) ds \ . \tag{3.26}$$

It can be shown that the right hand side

$$-\lim_{\epsilon\to 0^+} \int\limits_{\partial D_\epsilon} \left(\psi(x,y)\frac{\partial}{\partial n}G(x,y;\xi,\eta) - G(x,y;\xi,\eta)\frac{\partial}{\partial n}\psi(x,y)\right) = \frac{2m}{\hbar^2}\psi(\xi,\eta) \tag{3.27}$$

for the Green's function (3.22). The proof requires writing the Bessel functions in $G(x,y;\xi,\eta)$ as power series representations and Taylor expanding $\psi(x,y)$ about the point (ξ,η).[4] Using this fact, we can write the useful result

$$\frac{\hbar^2}{2m}\int\limits_{\partial D} \left[\psi(x,y)\frac{\partial}{\partial n}G(x,y;\xi,\eta) - G(x,y;\xi,\eta)\frac{\partial}{\partial n}\psi(x,y)\right] ds = \psi(\xi,\eta) \quad \text{if } (\xi,\eta)\in D \ . \tag{3.28}$$

If we know the Green's function, $\psi(x,y)$ and $\partial\psi/\partial n$ on the boundary, then we can find the solution inside the region.

In general, boundary value problems specify either $\psi(x,y)$ (*Dirichlet boundary condition*) or the normal derivative $\partial\psi/\partial n$ (*Neumann boundary condition*) on the boundary. The infinite potential well problems are significantly simpler than the general case because the boundary condition – $\psi(x,y) = 0$ everywhere on the boundary – gets rid of half of the integral in equation (3.28). However, we will continue discussing the general case.

[3] This is the standard choice when using Green's theorem. We used Green's theorem while deriving the reciprocal relations (when using the divergence theorem), so we follow this convention.

[4] Ang, W. T., *A Beginner's Course in Boundary Element Methods* (Universal Publishers, Boca Raton, 2007)

Third, let's look at the case $(\xi,\eta)\in\partial D$. For the same reason as before, we cannot use Green's function in the reciprocal relation on D since the Green's function does not satisfy our PDE at (ξ,η). We fix this problem by redefining the region as in Figure 3.1c. Take a disk of radius ϵ centered at (ξ,η), which we call D_ϵ, and exclude D_ϵ from D. The new region D'' does not contain (ξ,η), so we can use the reciprocal relation for $G(x,y;\xi,\eta)$ and the unknown solution $\psi(x,y)$. The boundary $\partial D''$ has two parts: C and C_ϵ where $C\subset\partial D$ and $C_\epsilon\subset\partial D_\epsilon$.

$$\int\limits_{\partial D''}\left(\psi\frac{\partial G}{\partial n}-G\frac{\partial\psi}{\partial n}\right)ds=\int\limits_{C}\left(\psi\frac{\partial G}{\partial n}-G\frac{\partial\psi}{\partial n}\right)ds+\int\limits_{C_\epsilon}\left(\psi\frac{\partial G}{\partial n}-G\frac{\partial\psi}{\partial n}\psi\right)ds=0\ . \tag{3.29}$$

Since this must hold for any disk of radius ϵ, take the limit $\epsilon\to0^+$:

$$\int\limits_{\partial D}\left(\psi\frac{\partial G}{\partial n}-G\frac{\partial\psi}{\partial n}\right)ds=-\lim_{\epsilon\to0^+}\int\limits_{C_\epsilon}\left(\psi\frac{\partial G}{\partial n}-G\frac{\partial\psi}{\partial n}\right)ds\ . \tag{3.30}$$

Note that we have used

$$\lim_{\epsilon\to0^+}\int\limits_{C}\left(\psi\frac{\partial G}{\partial n}-G\frac{\partial\psi}{\partial n}\right)ds=\int\limits_{\partial D}\left(\psi\frac{\partial G}{\partial n}-G\frac{\partial\psi}{\partial n}\right)ds\ . \tag{3.31}$$

To be precise, the integral on the right hand side does not exist because G has a singularity at $(\xi,\eta)\in\partial D$. However, we can *define* the value of the integral according to (3.31). This is the definition of *Cauchy principal value*.

Using the same method as before, we can show that

$$-\lim_{\epsilon\to0^+}\int\limits_{C_\epsilon}\left(\psi(x,y)\frac{\partial}{\partial n}G(x,y;\xi,\eta)-G(x,y;\xi,\eta)\frac{\partial}{\partial n}\psi(x,y)\right)ds=\frac{m}{\hbar^2}\psi(\xi,\eta)\ , \tag{3.32}$$

if (ξ,η) is on a smooth boundary.[5] Plugging this into (3.30), we obtain

$$\frac{\hbar^2}{2m}\int\limits_{\partial D}\left[\psi(x,y)\frac{\partial}{\partial n}G(x,y;\xi,\eta)-G(x,y;\xi,\eta)\frac{\partial}{\partial n}\psi(x,y)\right]ds=\frac{1}{2}\psi(\xi,\eta)\quad\text{if }(\xi,\eta)\in\partial D\ . \tag{3.33}$$

In summary,

$$\boxed{\frac{\hbar^2}{2m}\int\limits_{\partial D}\left[\psi(x,y)\frac{\partial}{\partial n}G(x,y;\xi,\eta)-G(x,y;\xi,\eta)\frac{\partial}{\partial n}\psi(x,y)\right]ds=\begin{cases}0 & \text{if }(\xi,\eta)\notin D\\ \psi(\xi,\eta) & \text{if }(\xi,\eta)\in D\\ \frac{1}{2}\psi(\xi,\eta) & \text{if }(\xi,\eta)\in\partial D\ .\end{cases}} \tag{3.34}$$

[5] Ang, ibid.

This integral equation, called *boundary integral equation* is the main result of the BEM. The solution inside the region of interest is written as an integral of boundary conditions and Green's function. The boundary integral equation is exact.

However, our task is not yet complete because we need to know both $\psi(x, y)$ and $\partial\psi/\partial n$ on the boundary to evaluate the left hand side of (3.34). In general, only one of $\psi(x, y)$ or $\partial\psi/\partial n$ is given for each point on the boundary. We still need to find the missing boundary condition (either ψ or $\partial\psi/\partial n$ for each point) to evaluate the integral. This can be done numerically in the following way.

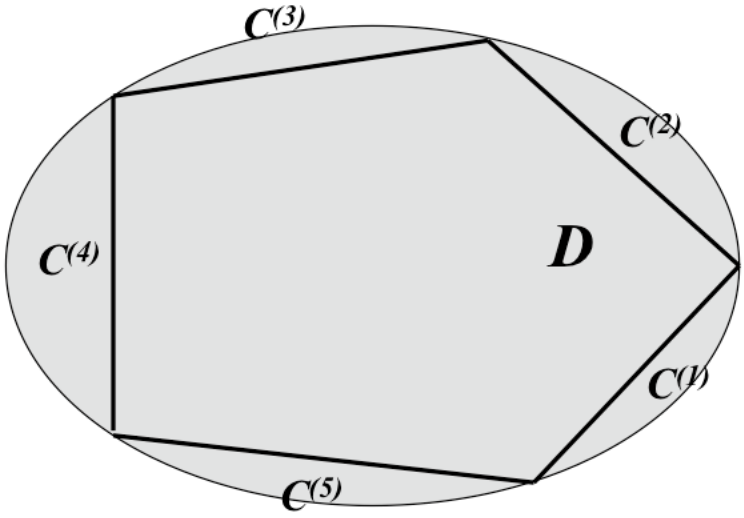

Figure 3.2: The boundary of D is discretized and approximated as a polygon (pentagon in this example).

We discretize the boundary and approximate it as a polygon with N sides (Figure 3.2). Call each side of the polygon $C^{(1)}, C^{(2)}, C^{(3)}, \cdots, C^{(N)}$. On each segment, approximate that the boundary conditions are constant:

$$\psi(x, y) \approx \overline{\psi^{(k)}} \quad \text{and} \quad \frac{\partial\psi(x, y)}{\partial n} \approx \overline{u^{(k)}} \quad \text{if } (x, y) \in C^{(k)} \ . \tag{3.35}$$

Apply (3.34) to the midpoint of $C^{(j)}$, which we call $\left(\overline{x}^{(j)}, \overline{y}^{(j)}\right)$:

$$\frac{1}{2}\overline{\psi^{(j)}} = \frac{\hbar^2}{m} \sum_{i=1}^{N} \left(\overline{\psi^{(i)}} \int\limits_{C^{(i)}} \frac{\partial}{\partial n} G(x, y; \overline{x}^{(j)}, \overline{y}^{(j)})\, ds - \overline{u^{(i)}} \int\limits_{C^{(i)}} G(x, y; \overline{x}^{(j)}, \overline{y}^{(j)})\, ds \right) \tag{3.36}$$

Note that since $\left(\overline{x}^{(k)}, \overline{y}^{(k)}\right)$ lies on the boundary, we are using the third case in (3.34). Also notice that while we are treating ψ and $\partial\psi/\partial n$ as constants on the boundary, the Green's function and its normal derivative still have to be integrated along each segment.

In order to simplify notation, define

$$A_{ij} \equiv \int\limits_{C^{(i)}} \frac{\partial}{\partial n} G(x, y; \overline{x}^{(j)}, \overline{y}^{(j)})\, ds \ , \quad B_{ij} \equiv \int\limits_{C^{(i)}} G(x, y; \overline{x}^{(j)}, \overline{y}^{(j)})\, ds \ . \tag{3.37}$$

In practice, A_{ij} and B_{ij} can be approximated by simple trapezoidal rule or Gaussian quadrature (or any other numerical method of choice). Using this definition,

$$\overline{\psi^{(j)}} = \frac{2\hbar^2}{m} \sum_{i=1}^{N} \left(\overline{\psi^{(i)}} A_{ij} - \overline{u^{(i)}} B_{ij} \right) \ . \tag{3.38}$$

Since we are given just one of $\overline{\psi^{(i)}}$ and $\overline{u^{(i)}}$, there are N unknowns on the right hand side. But we can generate N equations of this type for $j = 1, 2, 3, \cdots, N$. The problem is reduced to solving N linear equations. At this stage, we can hand this problem to a computer and get the missing boundary conditions. Once we find ψ and $\partial\psi/\partial n$ everywhere on the boundary, then we can find the solution to our PDE anywhere inside D using the boundary integral equation (3.34).

For the potential well problem, $\overline{\psi^{(i)}} = 0$ for every segment, so the missing boundary condition is $\overline{u^{(i)}}$. Using the given boundary condition, we get a considerably simpler equation

$$\sum_{i=1}^{N} B_{ij} \overline{u^{(i)}} = 0 \ , \tag{3.39}$$

which can be rewritten as a matrix-vector product

$$B\, \mathbf{u} = 0 \ , \tag{3.40}$$

where B is the $N \times N$ matrix with elements B_{ij} and $\mathbf{u} = (\overline{u}^{(1)}, \overline{u}^{(2)}, \overline{u}^{(3)}, \cdots, \overline{u}^{(N)})$. Substituting in the Green's function for the Schrödinger equation,[6]

$$\begin{aligned} B_{ij} &= \int\limits_{C^{(i)}} H_0^{(1)}(k\,|\mathbf{r} - \mathbf{r_j}|)\, d\mathbf{s} \\ &= \Delta s_i \int_{-\frac{1}{2}}^{\frac{1}{2}} H_0^{(1)}(k\,|\mathbf{r_i} + t\Delta\mathbf{s_i} - \mathbf{r_j}|)\, dt \ , \end{aligned} \tag{3.41}$$

[6]The multiplying constant in the Green's function has been excluded because we can divide or multiply both sides of (3.40) by any constant and get the same result.

where $\mathbf{r_i}$ and $\mathbf{r_j}$ are the midpoints of line segments $C^{(i)}$ and $C^{(j)}$, and $\Delta\mathbf{s_i}$ is the vector from the starting point of the line integral to the end point. The advantage of parametrizing the integral in this way is that we can easily estimate the integral using trapezoidal rule (length of the interval times the value at the midpoint):

$$\int_{-\frac{1}{2}}^{\frac{1}{2}} H_0^{(1)}(k\,|\mathbf{r_i} + t\Delta\mathbf{s_i} - \mathbf{r_j}|)\,dt \approx H_0^{(1)}(k\,|\mathbf{r_i} - \mathbf{r_j}|)\ , \tag{3.42}$$

so that

$$B_{ij} \approx \Delta s_i H_0^{(1)}(k\,|\mathbf{r_i} - \mathbf{r_j}|)\ . \tag{3.43}$$

However, there is a subtle problem. When $\mathbf{r_i} = \mathbf{r_j}$, the Hankel function is singular, which means all the diagonal elements of the matrix B are ill-defined. Nevertheless, we can estimate (3.42) in the Cauchy principal sense, i.e. changing the interval of the integral to $[-1/2, -\epsilon] \cup [+\epsilon, 1/2]$ and taking the limit $\epsilon \to 0$.

There is a simpler way of getting around this problem. For $\mathbf{r_j} \in \partial D$, we can define the directional derivative normal to the boundary at $\mathbf{r_j}$, which we shall call $\partial/\partial n_j$. The boundary integral equation is

$$-\frac{\hbar^2}{2m}\int_{\partial D} G(\mathbf{r_i};\mathbf{r_j})u(\mathbf{r_i})\,ds = \frac{1}{2}\psi(\mathbf{r_j})\ . \tag{3.44}$$

We can apply $\partial/\partial n_j$ to both sides, finding

$$-\frac{\hbar^2}{m}\int_{\partial D} \frac{\partial}{\partial n_j}G(\mathbf{r_i};\mathbf{r_j})u(\mathbf{r_i})\,ds = u(\mathbf{r_j})\ . \tag{3.45}$$

Using the explicit formula for the Green's function and the chain rule,[7]

$$u(\mathbf{r_j}) = -\frac{ik}{2}\int_{\partial D} \cos\phi_{ij} H_1^{(1)}(k\,|\mathbf{r_i} - \mathbf{r_j}|)u(\mathbf{r_i})\,ds, \tag{3.46}$$

where

$$\cos\phi_{ij} \equiv \hat{\mathbf{n}}_\mathbf{j} \cdot \frac{\mathbf{r_i} - \mathbf{r_j}}{|\mathbf{r_i} - \mathbf{r_j}|}\ . \tag{3.47}$$

Now repeat the same process of parametrizing the curve and using trapezoidal rule, giving

$$\boxed{u(\mathbf{r_j}) \approx -\frac{ik}{2}\sum_{i=1}^{N} u(\mathbf{r_i})\Delta s_i \cos\phi_{ij} H_1^{(1)}(k\,|\mathbf{r_i} - \mathbf{r_j}|)\ .} \tag{3.48}$$

[7] Kosztin and Schulten, ibid.

This is the equation for the computer to solve. There are N unknowns on the right hand side, and we can generate N equations for $j = 1, 2, 3, \cdots N$. Moving everything to one side,

$$\sum_{i=1}^{N} \left(\delta_{ij} + \frac{ik}{2} \Delta s_i \cos\phi_{ij} H_1^{(1)}(k\,|\mathbf{r_i} - \mathbf{r_j}|) \right) u(\mathbf{r_i}) = 0 \ , \tag{3.49}$$

$$\sum_{i=1}^{N} C_{ij} u(\mathbf{r_i}) = 0 \ . \tag{3.50}$$

This can be written as a matrix-vector multiplication:

$$C\,\mathbf{u} = 0 \ , \tag{3.51}$$

where $\mathbf{u} = (u(\mathbf{r_1}), u(\mathbf{r_2}), u(\mathbf{r_3}), \cdots, u(\mathbf{r_N}))$ and

$$C_{ij} \equiv \delta_{ij} + \frac{ik}{2} \Delta s_i \cos\phi_{ij} H_1^{(1)}(k\,|\mathbf{r_i} - \mathbf{r_j}|) \ . \tag{3.52}$$

When $\mathbf{r_i} = \mathbf{r_j}$, C_{ij} is no longer singular because $\cos\phi_{ij} = 0$ there. All the diagonal elements of C are just 1.

Once we have $\mathbf{u}$ by solving (3.51), we can use the boundary integral equation to find the solution inside the potential well.

$$\psi(\xi, \eta) = -\sum_{i=1}^{N} \overline{u}^{(i)} H_0^{(1)} \left(k \sqrt{(\overline{x}^{(i)} - \xi)^2 + (\overline{y}^{(i)} - \eta)^2} \right) \ . \tag{3.53}$$

3.4 Finding eigenvalues

Linear equations of the form (3.51) do not always have a nontrivial solution. The solution exists only when the matrix C is singular. In other words, we need $\det(C) = 0$. Since the matrix elements C_{ij} are functions of $k = \sqrt{2mE}/\hbar$, the condition $\det(C) = 0$ is essentially an equation of E. Solving it for k gives us the eigenvalues for the potential well problem.

But the determinant of C does not actually fall to zero because of the approximations we have made along the way, such as the discretization of the boundary and the use of trapezoidal rule when evaluating Green's function integral. Moreover, $\det(C)$ is not a simple polynomial of degree N, but a complicated function that includes the Hankel function. It is no easy task to find the roots of $\det(C)$.

There is an easier alternative. $|\det(C)|$, which is a function of the real variable k, assumes absolute minima at the zeros (it would be zero in the ideal case). If we plot $|\det(C)|$ as a function

of k, the local minima correspond to the roots. Figure 3.3 shows a plot of $|\det(C)|$ vs. k for the circular potential well whose boundary has been discretized into 60 segments. Local minima are obtained at the k values that correspond to eigenenergies through the relation $k = \sqrt{2mE}/\hbar$.

It is possible that we miss one of the eigenvalues if the scanning interval Δk is bigger than the spacing between two eigenvalues. The only way to prevent this from happening is to use a small enough scanning interval. It can be problematic at higher energies where the spacing between energies get smaller.

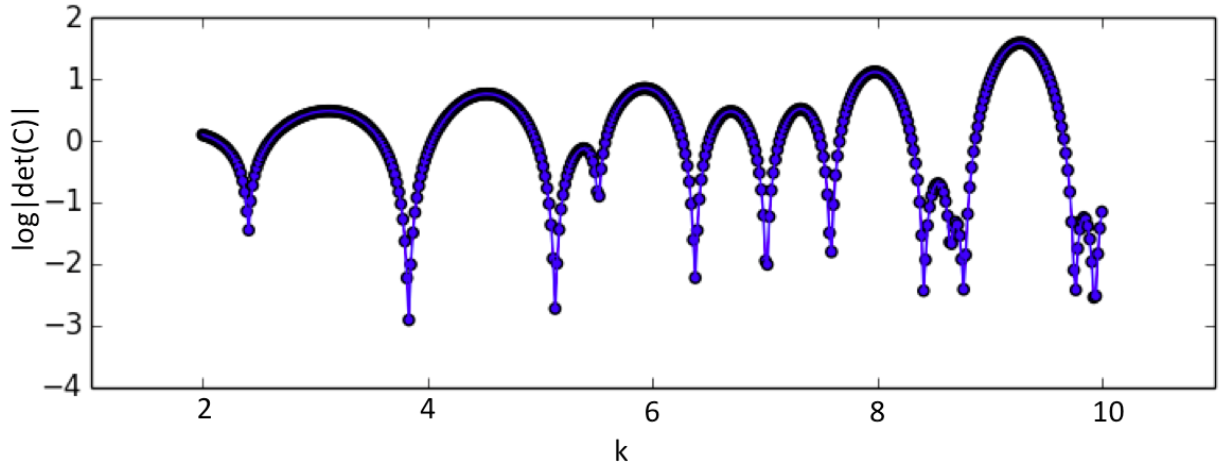

Figure 3.3: $\log|\det(C)|$ vs. k for the circular potential well with 60 discretization points. Energy eigenvalues can be calculated from the k values at local minima

Chapter 4

Modeling the Wells

The BEM can be used to find energy eigenvalues and eigenstates for potential wells of any shape, but let us first look at the square and circular wells, for which we have found analytic solutions in Chapter 2. We will then explore the case where the shape of the well changes continuously from circle to square.

4.1 Square well

The size of the square well we will consider is 1×1, where the units and constants are chosen so that $\hbar^2/(2m) = 1$. The energy eigenvalues are

$$E_{xy} = \pi^2(n_x^2 + n_y^2) \tag{4.1}$$

and the corresponding wavevectors are

$$k_{xy} = \pi\sqrt{n_x^2 + n_y^2}\ . \tag{4.2}$$

Table 4.1 compares the wavevectors k_{xy} calculated analytically from (4.2) and numerically from BEM. The boundary of the square was discretized into 80 segments for the application of BEM. The eigenvalues were first selected by taking the local minima from a $\log|\det(C)|$ vs. k graph that looks very much like Figure 3.3. Once the numbers were bracketed, the step size Δk was iteratively reduced small enough so that we have six significant figures after the decimal point. In all cases, the errors were less than 0.1%. There is no apparent relationship between error and energy level.

To find the energy eigenstate, we must first solve the matrix equation $C\mathbf{u} = 0$ and find $\mathbf{u}$. Then we can use (3.53) to calculate $\psi(\xi, \eta)$ anywhere inside the well. The problem $C\mathbf{u} = 0$ can be

Eigenenergy	n_x	n_y	k_{xy}	BEM	Error (%)
E_{11}	1	1	4.442883	4.442951	0.007
E_{12}	1	2	7.024815	7.024894	0.008
E_{22}	2	2	8.885766	8.885979	0.021
E_{13}	1	3	9.934588	9.934600	0.001
E_{23}	2	3	11.327173	11.327344	0.017
E_{14}	1	4	12.953118	12.953189	0.007
E_{33}	3	3	13.328645	13.328856	0.021
E_{24}	2	4	14.049629	14.049630	0.001

Table 4.1: Comparison of energy eigenvalues for the two dimensional infinite square well, computed analytically and through BEM. The boundary was discretized into 80 segments. In all cases, the errors are less than one part per thousand

phrased as finding a vector $\mathbf{u}$ in the null space of C. There are computer algorithms that solve this problem by singlar value decomposition. This is accomplished by using the linalg package of the NumPy extension to the Python programming language.

Figure 4.1 shows the energy eigenfunction for $n_x = 3$ and $n_y = 2$, computed from BEM. Compare this with the analytic solution in Figure 2.1. The 3×2 bumps are present, but are not of equal shapes as they are in the analytic solution. Considering that we get such high accuracy for eigenvalues, it is noteworthy that we do not get as accurate solution for the eigenfunction.

4.2 Circular well

Energy eigenvalues for the circular well can be found from the same method. Take a circular well of radius 1, where the constants are chosen so that $\hbar^2/(2m) = 1$. In this unit, wavevectors k_{nl} that correspond to eigenenergies E_{nl} are just the roots of Bessel functions of the first kind (See equation (2.27)).

For the square well, we looked at the error for different energy levels while keeping the number of discretization points the same. For the circular well, let's look at the error as a function of number of discretization points N, keeping the energy level constant as the ground state energy. We expect the error to decrease as N increases because the boundary can be approximated more accurately if there are more discretization points.

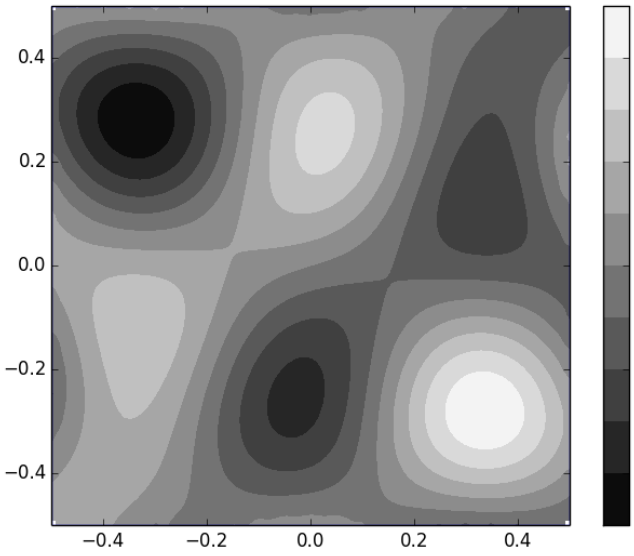

Figure 4.1: Energy eigenfunction for the square well, $n_x = 3$ and $n_y = 2$, found by BEM with 80 discretization points.

Figure 4.2 shows the relationship between error and N on a log scale. The blue line is the least-squares fit to the function

$$(\text{error}) = AN^p \ . \tag{4.3}$$

The fit function shows that the error falls off like $1/N^2$ for the ground state of the circular well.

One practical application of this remarkable result would be numerically estimating the roots of Bessel functions of the first kind. Assume that we do not know the value of the root. Pick a reasonably large number of discretization points (say 15) and find the eigenenergy using the $\log|\det(C)|$ vs. k plot. This estimate has some error (say ϵ) from the actual root. Now, double the number of discretization points (to 30) and estimate the eigenvalue again. This time, the error is reduced to one fourth of the original error ($\epsilon/4$). By taking the difference of the eigenvalues for the two discretization points, we can estimate the value of ϵ. Finally, subtract ϵ from the first estimate to get a new estimate that is closer to the actual value. For a better estimate, we can use more points.

The eigenstates for the circular potential well were plotted using the BEM. Figure 4.3 shows numerically computed eigenstates for the same n, l values we used in Figure 2.2. Notice that the ground state $n = 1$, $l = 0$ in the two figures have opposite signs. A more interesting feature is that

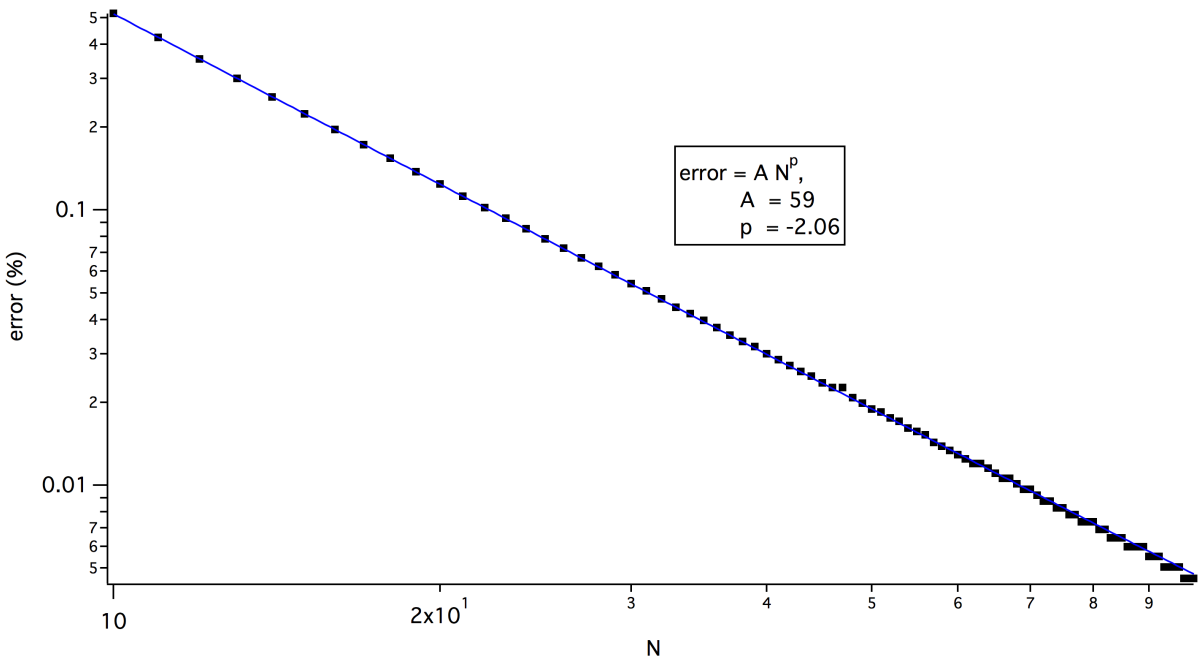

Figure 4.2: Error vs. N (number of discretization points) for the ground state of circular potential well

for the other three states, the solutions found from the BEM are the degenerate pairs for the ones in Figure 2.2.

4.3 Circular well to square well

How is symmetry related to degeneracy? A circle has infinitely many symmetry axes: any line passing through the origin. A square has four symmetry axes: the diagonals and the lines connecting opposing midpoints. For the circular potential well, every energy eigenvalue, except for the ground state, is doubly degenerate. For the square potential, there are infinitely many nondegenerate energy levels when $n_x = n_y$. Is it the case that the circular potential well has less nondegenerate states than the square potential has because the circle is more symmetric?

We investigate this problem by breaking the symmetry of the circle and slowly changing its shape to resemble a square. As we continuously change the shape of the well, we should somehow end up with infinitely many nondegenerate states. This cannot be done if all the degenerate energy levels of the circular well keep their degeneracies. At some point, the degeneracy has to be lifted. Let's follow the degeneracies of the circular energy levels to see how this happens.

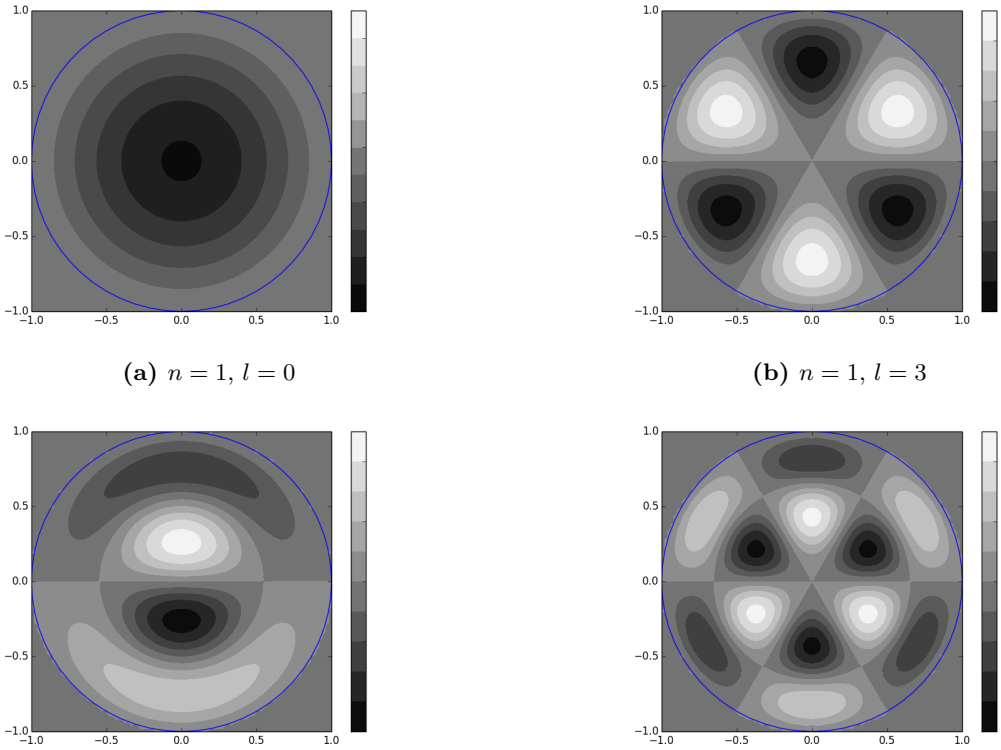

(a) $n = 1, l = 0$ **(b)** $n = 1, l = 3$

(c) $n = 2, l = 1$ **(d)** $n = 2, l = 3$

Figure 4.3: Contour plots of energy eigenfunctions for the infinite circular well of radius 1, calculated from the BEM.

The shape of the well was defined by the boundary $|x|^n + |y|^n = 1$, where $n \geq 2$. For each n, $\log|\det(C)|$ vs. k graph was generated and the k values corresponding to local minima were selected. The scanning interval Δn was 0.05. Once the energy eigenvalues[1] for each n from 2 to 11 were obtained, they were plotted for different values of n. The result is Figure 4.4.

Before we look at the details, notice that the eigenvalues for the circular potential well all tend to decrease at first. Also notice that this tendency is stronger for higher energy levels. A possible explanation, although not entirely rigorous because of the disappearance of degenereacies we will consider next, is that the set $\{n_x, n_y \in \mathbb{N} : \sqrt{n_x^2 + n_y^2}\}$ is denser than the set of roots of Bessel functions of the first kind. The latter defines where the eigenvalues are plotted on the left side of Figure 4.4. The former defines where the eigenvalues must arrive at the right end of the plot. If we

[1]To be precise, the *wavevectors* that correspond to energy eigenvalues were plotted, but we will use the terms interchangeably because one can be calculated from the other by just squaring or taking the square root.

have more eigenvalues on the right end than on the left end, we need to "pull down" the eigenvalues from the left. This is not a rigorous argument and its truth must be tested. But if this argument is valid, we can generalize the result and use it to compare the denseness of a pair of infinite sets, assuming the two sets can be expressed as limits of a continuously changing system.

Now let's look at magnified subsections of Figure 4.4, paying particular attention to the degeneracy of each state. Figure 4.5a shows the first two energy levels. The first level – the ground state of the circular well – is nondegenerate. The corresponding eigenvalue on the right is for $n_x = n_y = 1$, so it is also nondegenerate. The second level is doubly degenerate for both potentials. So far, everything makes sense.

Figure 4.5b shows the 3, 4, 5th energy levels. The third level on the left, like every other level for the circular well, is doubly degenerate. On the other hand, the third level on the right is for $n_x = n_y = 2$, so it is nondegenerate. Therefore, the degeneracy of the third level has to be lifted at some point. According to 4.5b, this seems to happen at the moment the symmetry of the circular potential is broken. When the third level splits into two levels, the lower level becomes the $n_x = n_y = 2$ state.

Meanwhile, the upper level, which is now nondegenerate, somehow has to disappear because otherwise we would have two nondegenerate states back to back. This is achieved by borrowing the degeneracy from the 4th level. The 4th level and the upper one of the split 3rd level merge together to form a *doubly* degenerate state. One degeneracy is lost in the process. In terms of eigenstates, the three corresponding eigenstates for these levels slowly change so that one of the three can be written as a linear combination of the other two. We expect this type of energy level merging whenever a degeneracy is lifted.

The fifth and sixth levels are not very interesting because they are doubly degenerate at both ends of the plot.

The seventh energy level splits into two and becomes the nondegenerate $n_x = n_y = 3$ level. As we expected earlier, the other half merges with another doubly degenerate state and forms a different doubly degenerate state eventually.

An important question to ask, which this thesis does not fully answer, is whether these merging and splitting of energy levels happen at the endpoints, i.e. at $n = 2$ and $n = \infty$, or at some other point in between.[2] If we confirm that energy splitting can happen for some $n > 2$, this is an evidence that not all degeneracies arise from symmetry since symmetry breaking happens only at

[2]It is perhaps unfortunate that we use n for two purposes: as in $|x|^n + |y|^n = 1$ and as a quantum number for the circular potential well.

$n = 2$. The four symmetry axes do not change during the rest of the process, so there is no change in terms of symmetry in between.

But there is another possible evidence that not all degeneracy comes from symmetry. The 9, 10, and 11th energy levels seem to cross each other. If they are in fact intersecting, the degeneracy of the states at the point of intersection is 4, assuming no degeneracy is lost because one can be expressed as linear combinations of others. Degeneracies of this type are not related to symmetry.[3]

[3]In fact, Michael Berry took a similar approach as this and found the so called "diabolical points" using triangular potential wells. See Berry, M. V. and Wilkinson, M. "Diabolical Points in the Spectra of Triangle" *Proc. R. Soc. Lond. A* **392** 15–43 (March 1984).

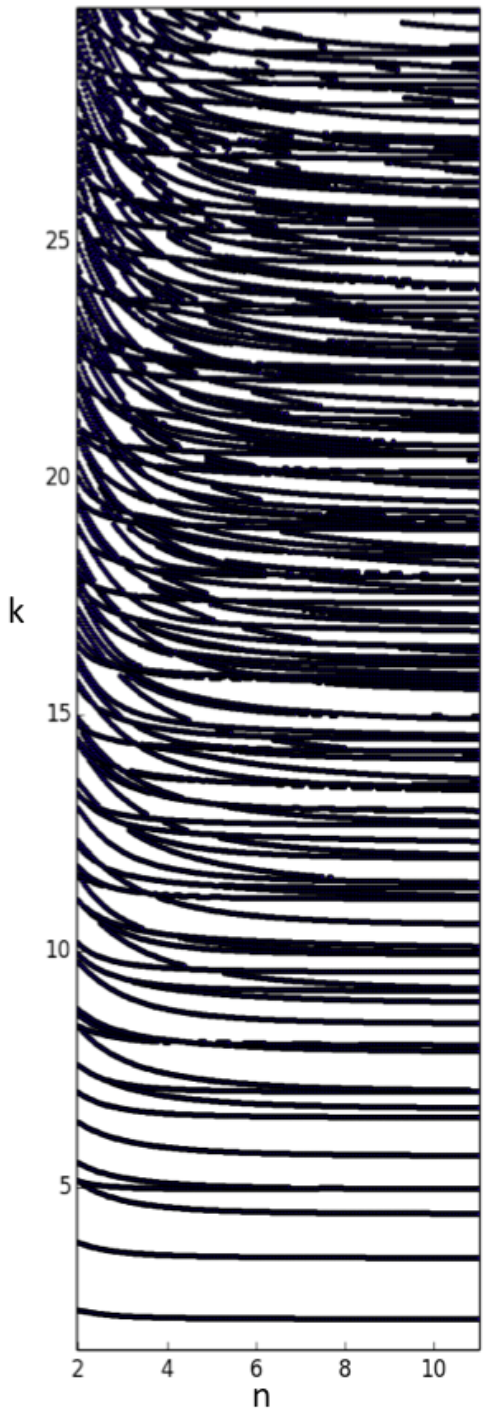

Figure 4.4: Energy eigenvalues for potential walls of $|x|^n + |y|^n = 1$, for $2 \leq n \leq 11$.

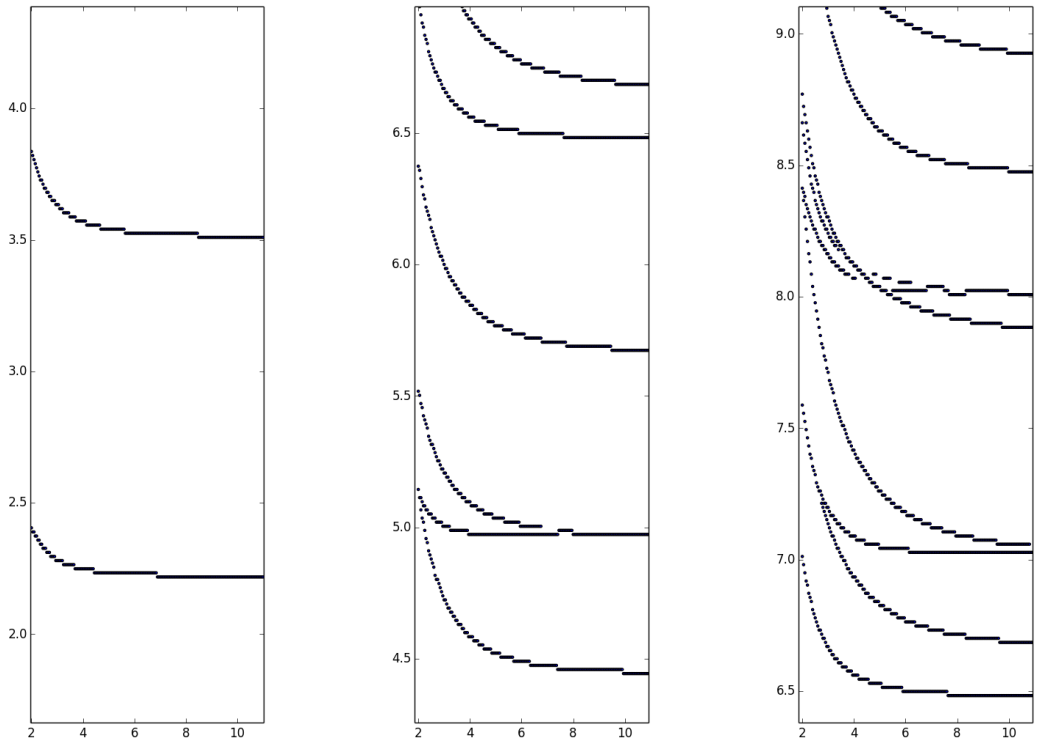

(a) The first two energy levels. **(b)** 3, 4, 5th energy levels. **(c)** 6, 7, 8th energy levels

Figure 4.5: Magnified subsections of Figure 4.4.

Chapter 5

Conclusion

Degeneracy is closely related to symmetry. Most symmetric systems, such as the circular or square potential wells, have degenerate energy levels. But we may wonder whether *every* degeneracy comes from symmetry. In an attempt to answer this question, we investigated potential wells of the type $|x|^n + |y|^n = a^n$, for $n \geq 2$.

We chose circular and square wells because we can find analytic solutions for these problems using separation of variables. The energy eigenvalues are related to the Bessel functions of the first kind and $\sqrt{n_x^2 + n_y^2}$, respectively.

The boundary element method (BEM) was used to numerically solve potential well problems. It uses the Green's function and the reciprocal relationship to express the solution inside the well as an integral of the Green's functions and its normal derivative. In order to test the reliability of the method, we compared numerical solutions from BEM to analytic solutions. When finding energy eigenvalues, errors of less than 0.1% could be easily achieved, whereas the eigenfunction for the square well was not as reliable. For the ground state of the circular well, error was found to be approximately proportional to $1/N^2$, where N is the number of discretization points. An approximation technique that exploits this property was proposed.

Energy eigenvalues for different values of n were plotted. We claimed that the downward initial slope of the eigenvalues was an evidence of the relative denseness of $\sqrt{n_x^2 + n_y^2}$ to the roots of the Bessel functions of the first kind. Each energy level was followed along the plot and its degeneracy was tracked. We found out that some degenerate states in the circular well split into two states of degeneracy 1. One of them becomes the nondegenerate energy level E_{nn} in the square well and the other merges with another degenerate level and disappears.

Future research may focus on determining whether the energy level splittings happen only at $n = 2$ or at some other values of n. If one confirms that it is possible to get an energy splitting at $n \neq N$, then this can be used as an evidence that not all degeneracies emerge from symmetry. Furthermore, the energy level crossings need to be studied in more depth because the points of intersection represent degenerate levels that arise without changes in symmetry.